0273-2289/88/1901—0071$06.20

Heterogeneous Modeling for the Alcoholic Fermentation Process

S. S. E. H. ELNASHAIE*,[1] AND G. IBRAHIM[2]

[1]Chem. Engng. Dept., King Saud Univ., Riyadh, P. O. Box 800, Saudi Arabia (On leave from the Chem. Engng. Dept., College of Engng., Cairo Univ., Egypt); and [2]Faculty of Engng., Menoufia Univ., Menoufia, Egypt

Received June 26, 1987; Accepted May 10, 1988

ABSTRACT

In this paper a heterogeneous model is developed for the alcoholic fermentation process. The model is expressed in terms of intracellular and extracellular concentrations of ethanol and sugar as well as biomass concentration as state variables. The model takes into consideration the floc size and the mass transfer rates of both ethanol and sugar. The intrinsic kinetics of the process used in the model was developed from published data which includes the inhibitory effects of ethanol and cells.

The model development is achieved through comparison with one set of experimental results given by Novak et al. (*1*). The model is then checked against two other sets of experimental results. The developed model is also used to simulate an industrial fed-batch fermentor.

NOMENCLATURE

A_p	External surface area of single floc	dm^2
A_{tf}	Total surface area of flocs	dm^2
D_p	Floc diameter	dm
K_{gs}	Mass transfer coefficient for sugar	dm/h
K_{gp}	Mass transfer coefficient for ethanol	dm/h
K_s	Saturation constant	g/L
$K_{p'}$	Inhibition constant	g/L
K_p	Rate constant	g/L
n	Toxic factor	dimensionless
P	Intracellular ethanol concentration	g/L
P_b	Extracellular ethanol concentration	g/L

*Author to whom all correspondence and reprint requests should be addressed.

R_p	Specific rate of ethanol production,	g ethanol produced/g dry wt of biomass.h
R_s	Specific rate of sugar consumption,	g sugar consumed/g dry wt of biomass.h
R_x	Specific growth rate	g biomass produced/g dry wt of biomass.h
r_p	Radius of floc	dm
S	Intracellular sugar concentration	g/L
S_b	Extracellular sugar concentration	g/L
S_o	Sugar concentration at initial condition	g/L
t	Time	h
V_b	Liquid volume of the bulk solution	L
V_t	Total (liquid + flocs) volume	L
V_{tf}	Total flocs volume	L
V_p	Volume of single floc	L
X	Biomass concentration	g dry wt/L
X_m	Maximum biomass concentration	g dry wt/L
Y_c	Yield factor for yeast,	g yeast produced/g sugar consumed
Y_p	Yield factor for ethanol,	g ethanol prod/g sugar consumed
Greek symbols		
μ_m	Maximum specific growth rate	h^{-1}
ρ	Density of floc	g dry wt/wet volume L

Index Entries: Alcoholic fermentation; ethanol; industrial fermentors; fed-batch fermentors; diffusion-reaction, heterogeneous modeling.

INTRODUCTION

Knowledge of biological reaction kinetics and mass transfer is essential for understanding the behavior of biological fermentors. However, in order to assemble a complete portrait of biological fermentor operation, it is necessary to consider the following fundamental phenomena and their complex interactions (*1–4*).

Product Inhibition

Several investigators studied the effect of ethanol on the specific rate of yeast growth and on the specific rate of ethanol production. The ethanol inhibition effect is of the noncompetitive type, where ethanol concentration affects only the maximum specific growth rate. The kinetic form by which ethanol concentration affects the maximum specific rates of growth and of ethanol production are markedly different. The dependence of the maximum specific rate of growth on ethanol concentration involves two main types of dependences: linear dependence (*3–4*), and nonlinear dependence (*5–7*). The underlying mechanisms are varying and quite complex (*8–10*). Jobses and Roels (*11*) have shown that inhibition kinetics can be approximated by a linear relation between the specific growth rate and the ethanol concentration up to 50 g/L ethanol. Above this level deviation from nonlinearity was observed.

Sugar Inhibition

It has been reported by several workers (*12–15*) that high sugar concentrations exhibit inhibitory effect on the growth of yeast and this was attributed to high osmotic pressure (*13–14*). Also a variety of nonfermentable sugars exhibit competitive inhibition (mainly monosaccharides) (*16*), when

polysaccharides containing media are used. Inhibitory effect of sugar is negligible below 100 g/L (*17*).

Cell Inhibition

In alcoholic fermentation most kinetic models express cell growth rate as a linear function of cell concentration. The experimental results of Cysewski and Wilke (*18*) and Lee et al. (*19*) showed that at high cell concentrations, the linear relationship is incorrect.

Transient Intracellular Accumulation of Ethanol

Nagodawithana and Steinkrous (*20*) reported that added ethanol was less toxic for the cell yeast (*Saccharomyces cerevisiae*) than ethanol produced by the yeast. They proposed that owing to an unbalance between the rate of production and the net outflux of ethanol there would be an intracellular accumulation of ethanol that in turn would explain the apparent greater inhibitory effect of produced ethanol. This hypothesis was supported by the findings of several authors (*21–25*). Novak et al. (*1*) measured the unsteady state intracellular and extracellular concentration of ethanol during the course of batch fermentation using *S. cerevisiae* strain UG5 from the ENSAT collection described by Strechaiano (*26*) and found a large difference between the intracellular and extracellular concentrations of ethanol during the early stages of fermentation, causing higher inhibition by ethanol at these early stages of fermentation. The findings of the above authors were recently challenged by Jobses and Roels (*11*) who were working with *zymomonas mobilis,* and by Guijarro and Lagunas (*27*) who were working with *S. cerevisiae* strains ATCC 42407 and ACA174 isolated from the must of an Andalusian wine (*28*).

Both groups (*11,27*) claim that concentration differences between intracellular and extracellular ethanol are negligible. Guijarro and Lagunas (*27*) claim that the difference between their results and the findings of previous investigators may be owing to inadequacy of the cell sampling procedure and the chromatographic conditions used by these investigators. It is also important to notice that Guijarro and Lagunas give results for batch fermentation where the extracellular concentration of ethanol is higher than the intracellular concentration. A detailed discussion of intracellular/extracellular ethanol concentration dispute is beyond the scope of the present paper. However, it is important to make it clear that the opinion of the authors of the present paper is that different results obtained by the different investigators are most probably not owing to inadequate analysis, as each group claims against the other but, in fact, the diffusion with chemical reaction is a complex phenomenon that may give different results under different conditions not only quantitatively but even qualitatively. This fact has been recognized in gas-solid catalytic systems after two decades of research (*29*).

Of course, the situation for diffusion and biochemical reaction in biological systems is even more complex, especially since none of the above-

mentioned contradictory results were carried out under similar conditions. The interaction between diffusion and biochemical reactions in such systems will depend upon many factors. This becomes clearer when the problem is treated rigorously, taking the following into consideration.

1. External mass transfer resistance, which depends upon the physical properties of the bulk fluid and the degree of mixing as well as temperature;
2. Diffusion through the cell membrane: a process that is not fully understood and that is affected by many factors (e.g., it is well known that ethanol increases the fluidity of biological membranes (*30*), besides, ethanol causes a change in the phospholipid composition and a decrease of the lipid to protein ratio of the membrane (*31*); and
3. Intracellular diffusion, which is dependent on the intracellular conditions (a rigorous description of the intracellular diffusion process may need a more structured diffusion-reaction model).

Also, the rate of mass transfer depends on the surface area for mass transfer, and this area is strongly affected by the flocculation phenomenon. The degree of flocculation varies with the strain of microorganisms (*32*) and also with the composition of the medium (*33*). Atkinson and Rahman (*34*) have investigated the diffusion limitation and its relation to floc size in the alcoholic fermentation process. In addition to all that, it has to be noted that the results of Novak et al. (*1*) are relating to the problem of transient diffusion with biochemical reactions, which introduces the extra parameter of the capacitance of the system. Although it has been well established for some time that the movement of ethanol across the plasma membrane is purely diffusional in nature (*35*), some of the results of both conflicting groups suggest that under certain conditions other transport mechanisms may be taking place (ref. *27*, Fig. 1, where the extracellular concentration of ethanol is higher than the intracellular concentration, and ref. *1*, Fig. 7, where for $t > 75$ h the extracellular concentration of ethanol is higher than the intracellular concentration).

The results of Novak et al. (*1*) for the concentration of ethanol in the intracellular and extracellular are used in the present paper to estimate some of the parameters of the developed heterogeneous model. The model with these parameters is used in the simulation of other experimental results as well as in the simulation of an industrial fed-batch fermentor.

MODEL DESCRIPTION

Although diffusion of sugar and ethanol through the cell wall and cell membrane plays an important role in alcoholic fermentation, little attention has been given to study the process as a diffusion-reaction system. This is most probably owing to the complexity and uncertainities associ-

ated with the diffusion and biochemical reaction for this system. In fact three main problems arise, related to the consideration of alcoholic fermentation as a diffusion reaction system.

Measurement of the Mass Transfer Coefficient for Ethanol Transport from the Intracellular to the Extracellular Fluid

Different investigators give very different estimations of this mass transfer coefficient. Virgillio and Ferreira (*41*) give a value of 0.36 m/h; Guijarro and Lagunas (*27*) estimate the value to be 0.0108 m/h; while Jobses and Roels (*11*) give two very different estimates calculated by two different methods. The first value is very high (6.12 m/h) and is based on the assumption that diffusion of ethanol through water layer is rate determining, the other estimated value in the same paper is 0.000745 m/h. In this study we use a value of ethanol mass transfer coefficient that is varying with sugar concentration and is obtained from the difference between intracellular and extracellular ethanol concentrations reported in Novak et al. work (*1*). The mass transfer coefficients are obtained by the method described in Appendix 1 and are fitted to a simple polynomial as a function of sugar concentration. The values of ethanol mass transfer coefficient obtained by this method vary between 0.000103 and 0.002253 dm/h.

Flocculation of the Yeast Cells

The flocculation affects strongly the area of mass transfer and thus the rate of growth and ethanol production. The rate of flocculation is affected by a great number of factors including even the strain of a certain yeast (*32*).

For *Saccharomyces cerevisiae* some strains have a strong flocculating tendency, whereas some other strains are nonflocculant. However, flocculation in nonflocculant strains may be induced by certain additives and certain pH values (*36,37*). Atkinson and Daoud (*38*) reported that the presence of certain chemical elements and compounds in the medium affect flocculation. Mill (*33*) confirmed the findings of Eddy (*39*) that certain specific sugars could disperse flocculent yeast. It has also been observed (*33,40*) that the presence of some nitrogeneous nutrients in the medium could delay the point in the growth cycle at which brewer's yeast becomes potentially flocculent.

Rainbow (*41*) confirmed the results of Mill (*33*) and Eddy (*39*) that certain fermentable sugars prevent flocculation or cause redispersal of flocculated yeast, but also reports a list of other substances that cause flocculation (furfural, a polysaccharide material "treberin," proteins, humic acid, melanodins, phlobaphene, and ethanol).

From this brief review, it is clear that the flocculation process is quite complex and is affected by many variables, and since flocculation affects the rate of mass transfer because of the change of mass transfer area,

these facts contribute to the explanation of the discrepancy between the results of different investigators with regard to the intracellular-extracellular ethanol concentration dispute discussed earlier. Jones et al. (*42*) used a mutant of *S. cerevisiae* in a tower fermentor with high sugar concentration and maintained high concentration of microorganisms. These results indicated the presence of mass transfer resistance within the tower fermentor yeast bed. In the present paper a constant floc size throughout the fermentation process is used. This floc size is obtained experimentally as discussed in Appendix 2.

Ethanol Inhibition Constant

As discussed earlier, many investigators reported that produced ethanol (intracellular ethanol) is more toxic than added ethanol (extracellular ethanol) (*1,20–25*). This is because of the fact that inhibition is usually correlated to the measured concentration of extracellular ethanol, therefore the inhibition effect of added ethanol is expected to be underestimated in comparison with the true inhibition, whereas that of produced ethanol is expected to be overestimated. Novak et al. (*1*) report an inhibition constant kp of 105.2 g/L for added ethanol and 3.04 g/L for produced ethanol. Based on the above understanding, it is expected that the true kp to be used in the heterogeneous model should have an intermediate value between the two mentioned values. In the present model, an intermediate value of kp was obtained by fitting the heterogeneous model to one set of the results of Novak et al. (*1*).

SINGLE FLOC MODEL

The single floc model used in this study consists of flocs of spherical shape (Fig. 1). It may be regarded as a substrate sink, a metabolic zone that is a region where the substrate is consumed and the product produced by the process of metabolism and a boundary region across which the substrate diffuses to react and the product diffuses out of the floc.

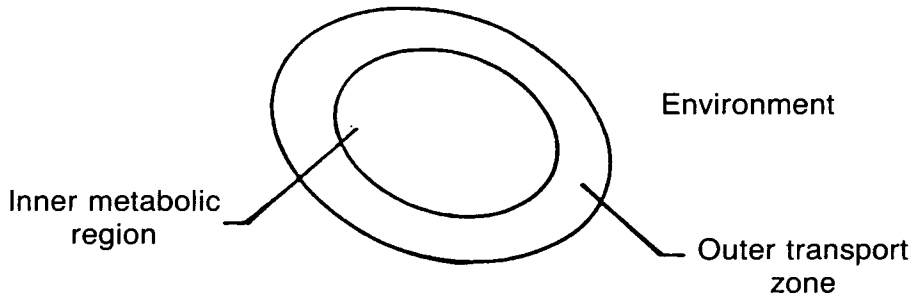

Fig. 1. A model for a single floc.

Basic Model Assumptions

In order to describe the model in mathematical terms, it is necessary to make a number of assumptions with regard to the characteristics of the microbial mass.

1. The cell is a unit whose functions are invariant with time and which has gross properties that are functions of the local environment;
2. For the microbial mass as a whole, the age distribution of the population and such properties as viability and adaptation are invariant with time;
3. All the mass transfer resistances are lumped in one hypothetical resistance layer and the diffusion through this layer obeys Fick's law of diffusion for both sugar and ethanol.

Single Floc Equations

From component material balance on sugar (S), the flux of sugar entering the inner metabolic zone of the single floc is equal to the rate of sugar uptake in this confined space (V_p) in addition to the rate of sugar accumulation within the metabolic zone

$$V_p \cdot dS/dt = A_p K_{gs} (S_b - S) - R_s \cdot \rho \cdot V_p \quad (1)$$

R_s is the specific sugar uptake rate in g of sugar consumed/g of dry wt of floc hr.

After some rearrangement we obtain

$$dS/dt = 6 K_{gs} (S_b - S) / D_p - R_s \cdot \rho \quad (2)$$

where D_p is the floc diameter.

For component material balance on the intracellular ethanol (P), the flux of ethanol through the metabolic zone of the single floc is equal to the ethanol production rate within the metabolic zone, minus the rate of ethanol accumulation within the floc.

$$dP/dt = - 6 K_{gp} (P - P_b) / D_p + R_p \cdot \rho \quad (3)$$

where R_p is the specific ethanol production rate in g ethanol produced/g of dry wt of floc h.

Bulk Solution Equations

The variation of sugar amount in bulk phase is equal to the overall rate of sugar removal. This equality is given by

$$d(S_b V_b) / dt = - A_{tf} K_{gs} (S_b - S) \quad (4)$$

where

$$d(S_b V_b) / dt = S_b (dV_b / dt) + V_b (dS_b / dt)$$

In the case of small microbial concentrations, the value (dV_b / dt) may be neglected, and Eq. (4) becomes

$$V_b\,(dS_b / dt) = -A_{tf} \cdot K_{gs} \cdot (S_b - S) \tag{5}$$

Similarly, the equation representing the variation of ethanol concentration in bulk phase is

$$V_b\,(dP_b / dt) = A_{tf}\,K_{gp}\,(P - P_b) \tag{6}$$

and the variation of biomass concentration with time is given by

$$V_t\,(dX / dt) = R_x\,X\,V_t \tag{7}$$

Thus

$$dX / dt = R_x\,X \tag{8}$$

where R_x is the specific growth rate in g of microorganisms produced/g dry wt of microorganisms h

The total mass transfer area can be calculated as follows. The total wet volume of flocs is

$$V_{tf} = X\,V_t / \rho \tag{9}$$

The total liquid volume is

$$V_t = V_b + V_{tf} \tag{10}$$

or

$$V_b = V_t - V_{tf} \tag{11}$$

According to the assumption of spherical shape, we obtain

$$V_{tf} = \pi \cdot N\,D_p^3 / 6 \tag{12}$$

where N is the total number of flocs of equal sizes. Equating Eqs. (9) and (12), we get

$$N = 6\,X\,V_t / (\rho \cdot \pi \cdot D_p^3) \tag{13}$$

The total mass transfer area is

$$A_{tf} = \pi \cdot D_p^2\,N \tag{14}$$

Thus

$$A_{tf} = \pi\,(D_p^2\,(6\,X\,V_t) / (\rho \cdot \pi \cdot D_p^3) = 6\,X\,V_t / (\rho \cdot D_p) \tag{15}$$

Dividing Eq. (5) by V_b and substituting from Eq. (11), the following equation is obtained

$$dS_b / dt = -A_{tf}\,K_{gs}\,(S_b - S) / (V_t - V_{tf})$$

Substituting from Eqs. (9) and (15), the following equation is obtained

$$dS_b / dt = -\,6\,X\,K_{gs}\,(S_b - S) / (D_p\,(\rho - X)) \tag{16}$$

Following the same procedure with Eq. (6), we obtain

$$dP_b / dt = 6 X K_{gp} (P - P_b) / (D_p (\rho - X)) \quad (17)$$

Kinetic Rate Equations

The equations for the reaction rates R_s, R_p, R_x take many forms. A detailed investigation and comparison between different kinetic rate expressions was carried out (*43*) before it was decided to use three main forms in this investigation.

The first pattern uses the kinetics developed by Egamberdiev (*6*) with the following kinetic rate equations

$$R_x = \mu_m K_p S / ((K_p + P)(K_s + S))$$
$$R_s = R_x / Y_c$$

and

$$R_p = Y_p R_s \quad (18)$$

Equation (18) does not include the yeast cells inhibition effect.

The second kinetic pattern used in this investigation is a modification of the above rate equation where the effect of the cell inhibition is introduced by a formula similar to the one used by Lee (*19*). The equations are

$$R_x = \mu_m K_p S(1 - X / X_m)^n / ((K_p + P)(K_s + S))$$
$$R_s = R_x / Y_c$$

and

$$R_p = Y_p R_s \quad (19)$$

A third kinetic pattern have been used by other workers (*5,12,45*) with two independent equations to represent R_x and R_p. However, this kinetic rate equation introduces new kinetic parameters that complicate the kinetics considerably. In this paper we have introduced a new equation with only one additional parameter, as follows

$$R_x = \mu_m K_p S(1 - X / X_m)^n / ((K_p + P)(K_s + S)) \quad (20)$$
$$R_s = 1 / Y_c [R_x + \mu_m K'_p / (K'_p + P)] \quad (21)$$
$$R_p = R_s Y_p$$

The additional term $\mu_m \cdot K'_p / (K'_p + P)$ means that the sugar consumption does not stop when the yeast growth stops ($R_s \neq 0$ when $R_x = 0$). These kinetic formulae were used subsequently in the development of the heterogeneous model that best fits one set of the unsteady state fermentation results of Novak et al. (*1*).

The initial value nonlinear differential equations for the different models presented in this paper are solved using the fourth order Runge-Kutta method with variable step size to ensure the numerical accuracy of the results.

RESULTS AND DISCUSSION

The Simplest Model

In this section the results of solving the heterogeneous model for Novak's batch fermentor (*1*) are presented. The kinetic rate equations described by Eq. (18) are used in the model and a constant value for ethanol mass transfer coefficient is assumed. The floc diameter is taken equal to 0.005 cm, which is about 5 times the usual industrial volume because of the absence of antifloculating agents. Figures 2–5 represent the results of

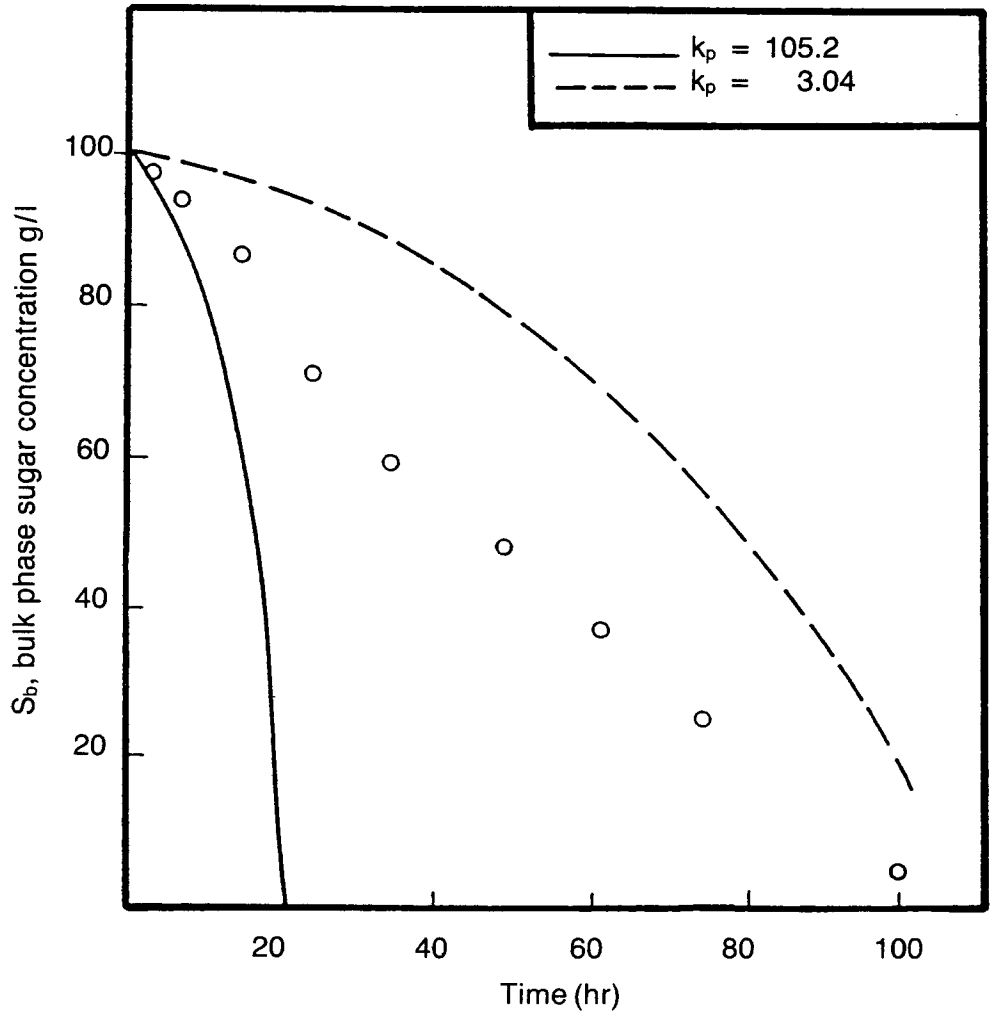

Fig. 2. Solution of the heterogeneous model using different K_p values and constant ethanol permeability. Extracellular sugar concentration vs time. ———— K_p=105.2 based on alcohol added. — — — — K_p=3.04 based on alcohol produced. ○○○○ Experimental data.

the batch fermentor with the above conditions. The theoretical response of the fermentor is shown for two values of the ethanol inhibition constant.

K_p = 105.2 g/L (based on alcohol added as given by Novak et al. (*1*))

and

K_p = 3.04 g/L (based on alcohol produced as given by Novak et al. (*1*))

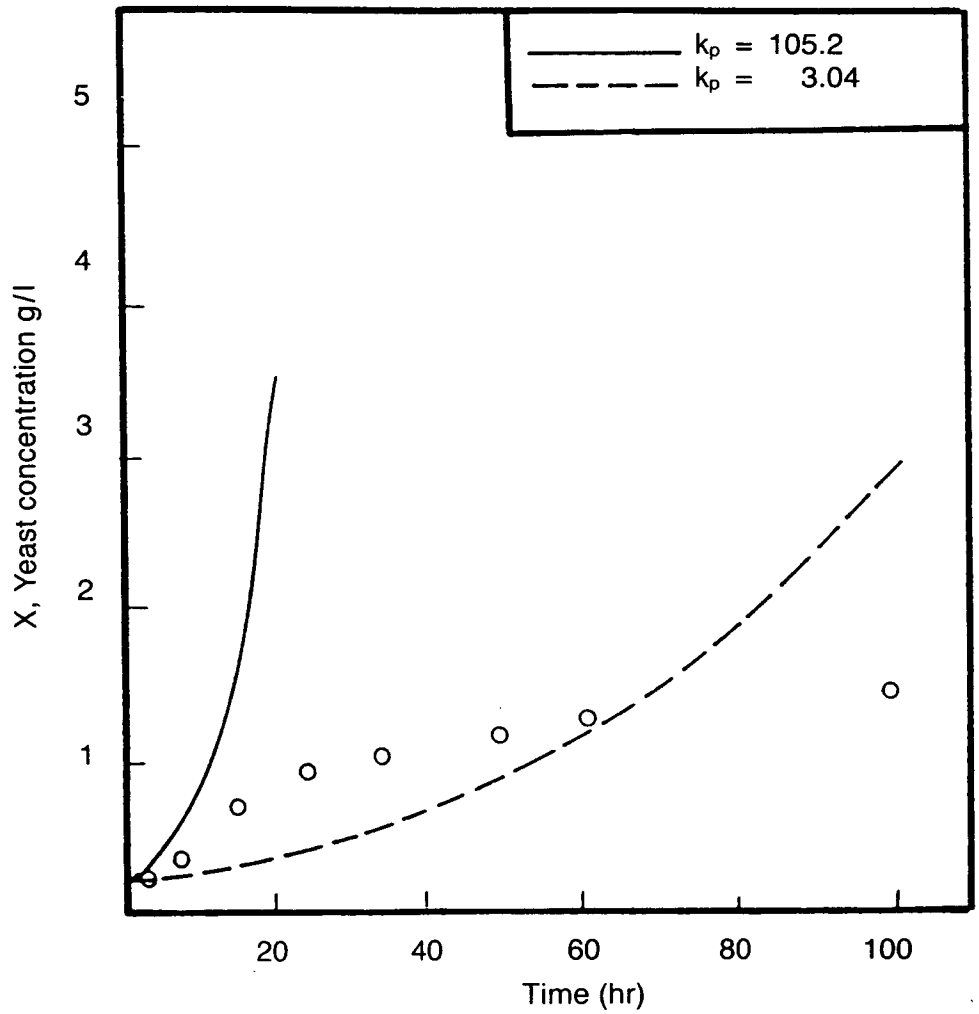

Fig. 3. Solution of the heterogeneous model using different K_p values and constant ethanol permeability. Biomass concentration vs time. ——— K_p=105.2 based on alcohol added. — — — — K_p=3.04 based on alcohol produced. ○○○○ Experimental data.

It is evident from Fig. 2 that, when $K_p = 105.2$ is used, the sugar uptake rate is very high and the fermentation time decreases to about one-fifth of the actual fermentation time. When the value of K_p used is 3.04, the sugar uptake rate is much slower than the actual rate and the fermentation time is more than the actual fermentation time. These results suggest the use of an intermediate value for K_p.

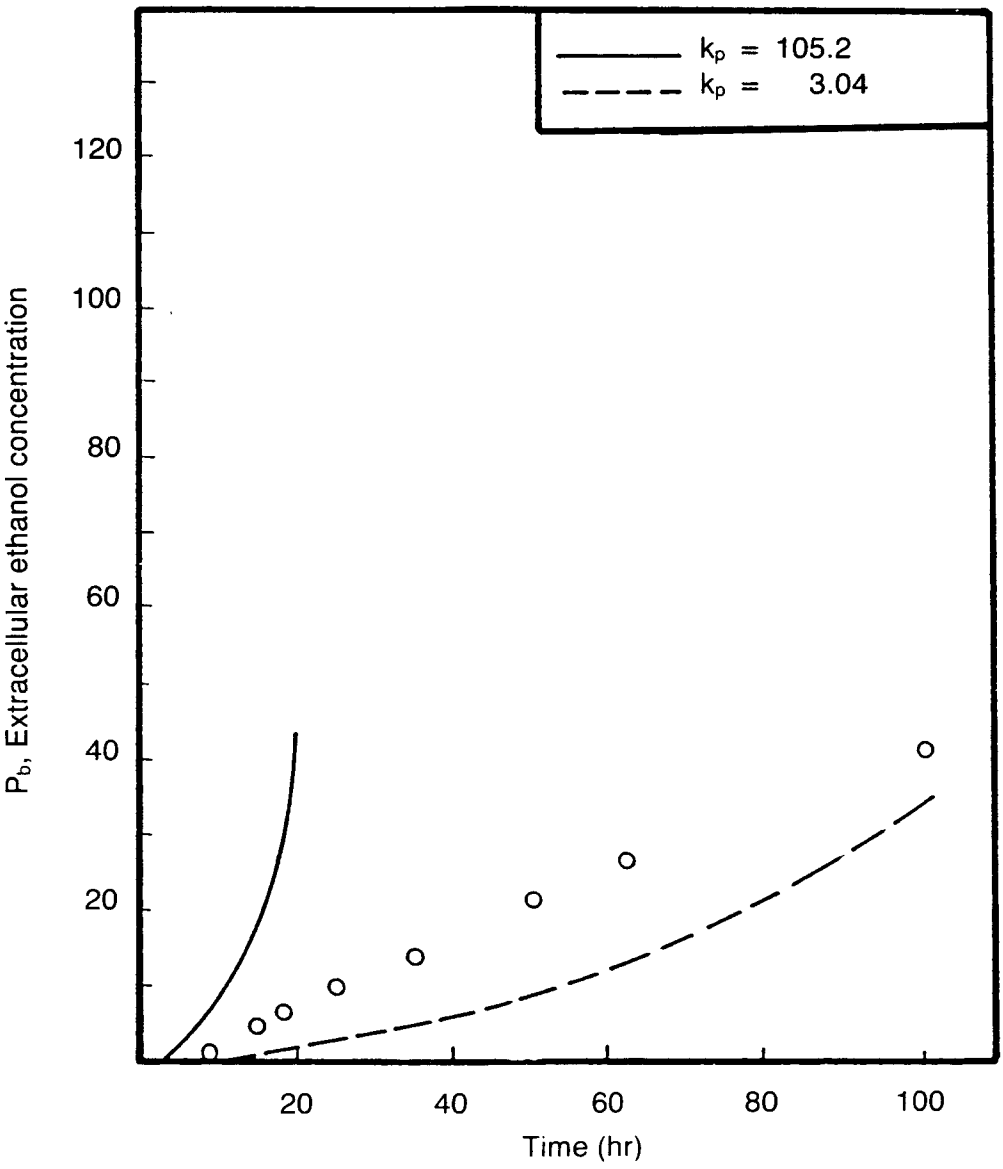

Fig. 4. Solution of the heterogeneous model using different K_p values and constant ethanol permeability. Extracellular ethanol concentration vs time. ——— $K_p = 105.2$ based on alcohol added. — — — — $K_p = 3.04$ based on alcohol produced. ○○○○ Experimental data.

For the case of $K_p = 3.04$, it is evident that the phenomenon of the overestimation of yeast production after a certain time (Fig. 3) cannot be explained on the same basis. However, we should notice that the kinetic rate equation used in this case does not include any term representing the death rate. This result obviously suggests the inclusion of a term for the death rate of cells.

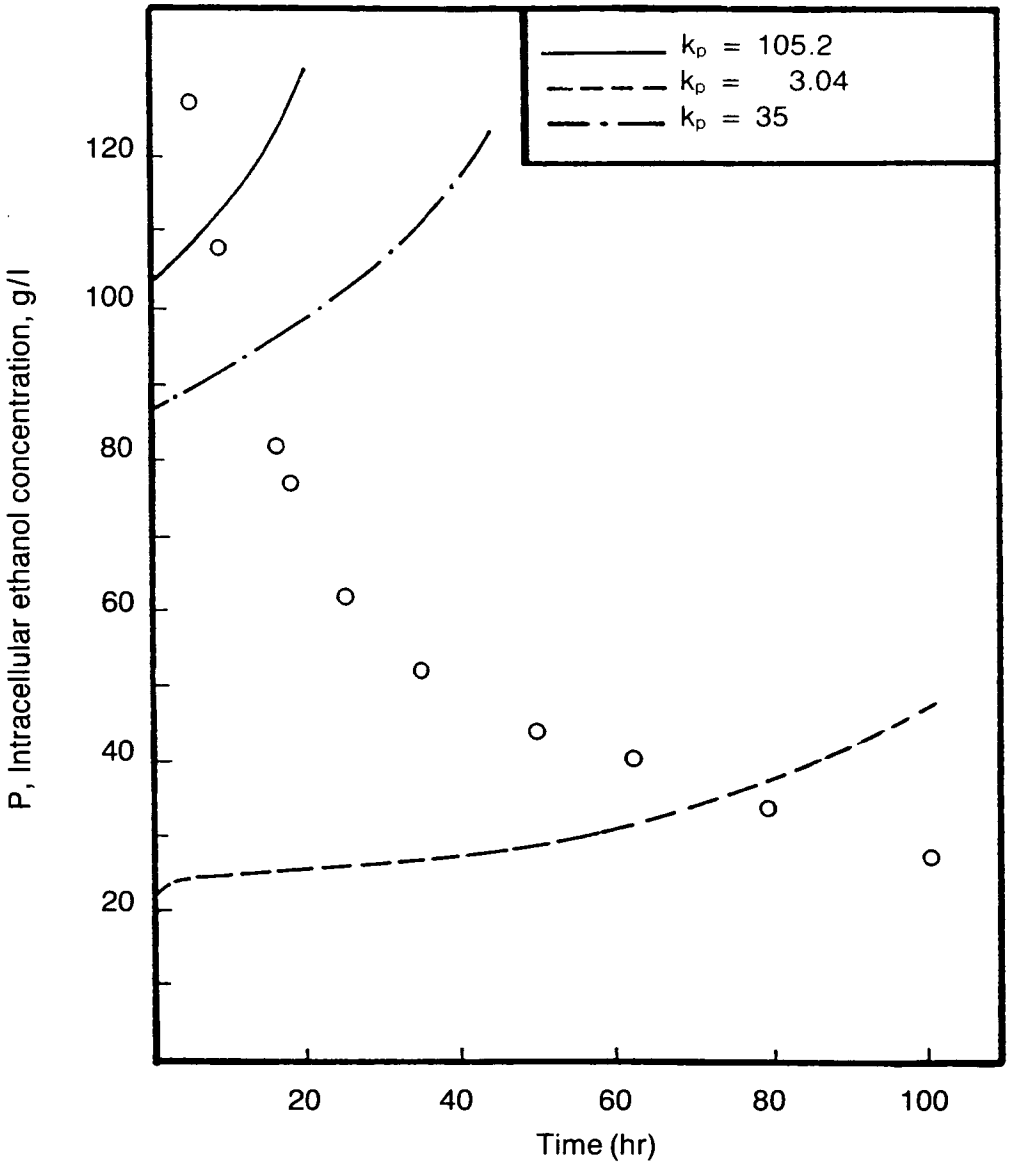

Fig. 5. Solution of the heterogeneous model using different K_p values and constant ethanol permeability. Intracellular ethanol concentration vs time. ———— $K_p = 105.2$ based on alcohol added. — — — — $K_p = 3.04$ based on alcohol produced. ○○○○ Experimental data. — —·— — $K_p = 35$.

Figure 4 represents the variation of the extracellular ethanol concentration vs time. It is evident that the use of $K_p = 105.2$ leads to high ethanol production rates, whereas the use of $K_p = 3.04$ leads to low rates relative to the experimental results. This again suggests the use of an intermediate value for K_p.

Figure 5 represents the variation of the intracellular ethanol concentration vs time. The results of this figure can be interpreted on the same basis as above, however, another important observation can be drawn from this figure. The theoretical curves do not exhibit a maximum in the wide time region considered, whereas the experimental results show a maximum intracellular ethanol concentration at a time of 3 h and a concentration of 127 gm/L. At $t > 3$ h, the intracellular concentration of ethanol decreases. Many trials to fit the nonmonotonic intracellular ethanol concentration using intermediate values of K_p were not fully successful. This implies that further modification of the model is required.

The early maximum of the intracellular ethanol concentration, as shown by the experimental results, is most probably owing to the change of ethanol mass transfer coefficient with conversion.

Estimation of Ethanol Mass Transfer Coefficient as a Function of Sugar Concentration

The method used to estimate ethanol mass transfer coefficient as a function of sugar concentration, is discussed in Appendix 1. The mass transfer coefficient changes from a value of $1.0858 * 10^{-5}$ m/h to a value of $22.536 * 10^{-5}$ m/h through the fermentation course. A polynomial is fitted to the results to express ethanol mass transfer coefficient as a function of sugar concentration (Appendix 1).

Model Development

From the observations and the analysis of differences between experimental results and the simplest model predictions in the previous section, it was concluded that the simple starting model should be improved in four directions.

1. Using an intermediate value of the inhibition constant;
2. Using a varying mass transfer coefficient for the ethanol;
3. Taking into consideration the death rate of the cells by including the term $(1 - X / X_m)^n$ presented by Lee (*18*). The specific growth rate, according to this variation, is given by Eq. (19). The value of X_m at the operating conditions of Novak et al. (*1*) is 1.5 g dry wt/L (at 100 g/L of sugar concentration at the beginning of fermentation), and n is taken as 1.7.
4. The equation representing the specific rate of growth must be separated from the equation representing the sugar uptake rate, i.e., kinetic expressions are used that involve two independent rate equations, one representing the specific rate of growth of microorganisms and the other representing the rate

of sugar uptake, whereas the rate of ethanol production is related to the sugar uptake equation by the stoichiometric ratio Y_p.

In addition a new term with one kinetic parameter is added to Eq. (19) to represent the rate of sugar uptake whenever $X \rightarrow X_m$. The kinetic pattern obtained is given by Eqs. (20,21). The new term means that even when the yeast growth stops, the rate of sugar uptake (and ethanol production) is not equal to zero. This is in accordance with the actual process. The simulation results that best fit Novak et al. (*1*) first set of experimental results are achieved by the use of this kinetic pattern (Eqs. (20,21) with the heterogeneous model represented by Eqs. (2,3,4,8,16,17), for the system of parameters summarized in Table 1. Figure 6 gives the variation of sugar concentration in bulk phase vs. time. Figure 7 gives the variation of extracellular ethanol concentration vs time. Figure 8 gives the variation of biomass concentration with time. Figure 9 gives the intracellular ethanol concentration variation with time.

It is clear from Figs. 6–9 that the developed heterogeneous model fits very well the behavior of the system.

Heterogeneous Model Testing

The above-mentioned modeling procedure has involved few parameters fitting to the one set of the experimental results of Novak et al. (*1*). Therefore, in order to test the validity of the developed heterogeneous model for other cases, the model was used to simulate other sets of experimental results given by Novak et al. (*1*).

Table 1
System Parameters Used in the Stimulation of Novak et al. (*1*)
First Set of Experimental Data

Parameter kind	Parameter symbol	Values of the parameters		Reference
Kinetic parameters	μ_m	0.313	h^{-1}	(*1*)
	K_p	35	g/L	—[a]
	X_m	1.5	g/L	(*1*)
	n	1.7	dimensionless	(*43*)
	K_s	0.22	g/L	(*5*)
	$K_{p'}$	3	g/L	—[a]
	Y_c	0.035	dimensionless	(*1*)
	Y_p	0.42	dimensionless	(*1*)
Physical parameters	D_p	5×10^{-4} dm		Appendix 2
	K_{gs}	5.04×10^{-2} dm/h		(*38,49*)
	ρ	200 g dry wt/L wet vol		(*1*)
	K_{gp}	Eq. (A.1) dm/h		Appendix 1

[a]Empirical fitting using Novak et al. (*1*) unsteady state experimental results.

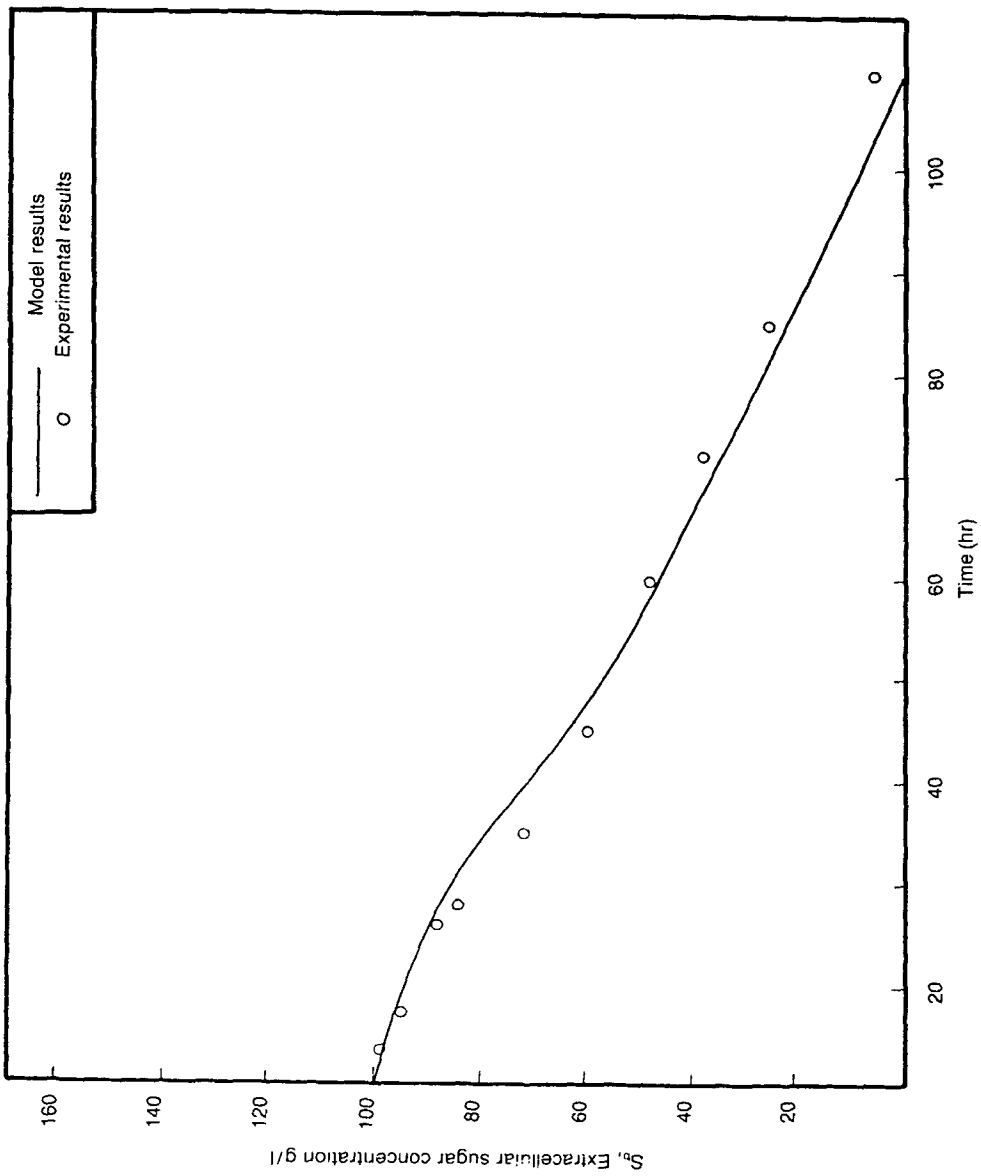

Fig. 6. Solution of the heterogeneous model using intermediate K_p value, variable ethanol permeability, cell inhibition effect, and two independent rate equations. Extracellular sugar concentration vs time.

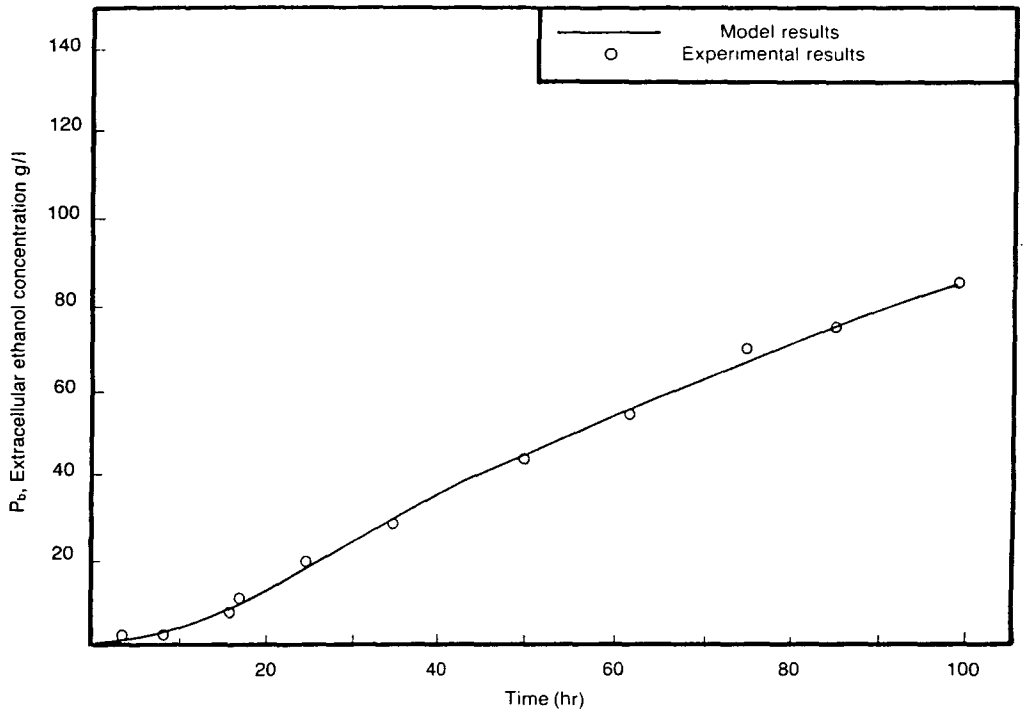

Fig. 7. Solution of the heterogeneous model using intermediate K_p value, variable ethanol permeability, cell inhibition effect, and two independent rate equations. Extracellular ethanol concentration vs time.

Novak et al. (*1*) measured the response of their fermentor (20 L in volume) when the sugar concentration in the feed was 80 g/L and 125 g/L. In these experiments they presented only the variation of the biomass and the extracellular ethanol concentrations with time. Figures 10 and 11 show that the developed heterogeneous model gives good agreement with the experimental results for biomass and extracellular ethanol concentration profiles for the two values of feed sugar concentrations. This test of the model against experimental results other than the one for which the model was fitted to obtain the parameters, demonstrate the validity of the model for the simulation and design of the fermentation process.

Comparison between the PseudoHomogeneous and the Heterogeneous Models

Figure 12 presents the response of both the pseudohomogeneous model defined by the equations

$$dS / dt = R_s X;\ dP / dt = R_p X;\ dX / dt = R_x X \qquad (23)$$

and the heterogeneous model for the kinetic pattern defined by Eqs. (20, 21), which are used in both cases. It is evident that the fermentation time predicted by the use of the pseudohomogeneous model is half the fermen-

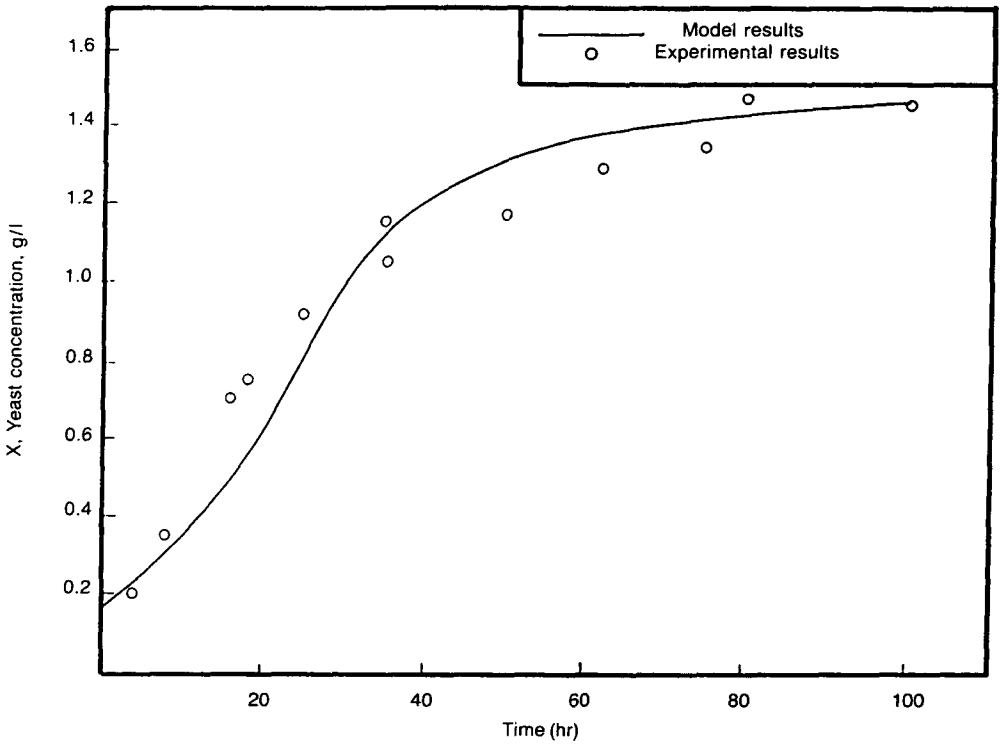

Fig. 8. Solution of the heterogeneous model using intermediate K_p value, variable ethanol permeability, cell inhibition effect, and two independent rate equations. Biomass concentration vs time.

tation time predicted by the use of the heterogeneous model. This again shows the importance of using the heterogeneous model developed in this paper rather than pseudohomogeneous models.

Industrial Fed-Batch Fermentor

An additional check of the model is carried out by comparing the model predictions against the performance of an industrial fed-batch fermentor. The model equations are modified to account for the fed-batch mode of operation (*40*).

The industrial fermentor under consideration operates under aerobic conditions for a period of 6–8 h in order to grow the necessary initial amount of yeast. Then it operates under anarobic fed-batch conditions until the liquid volume of the fermentor reaches the working volume of the fermentor (65000 L). This period ranges from 11 to 12 h. After this period, the fermentor operates under batch conditions for a period ranging from 6 to 8 h until the fermentable sugar is consumed.

The objective of this part is to simulate the anarobic period that constitutes about 76% of the total fermentation time, using the heterogeneous model developed earlier in order to present an extra check for the

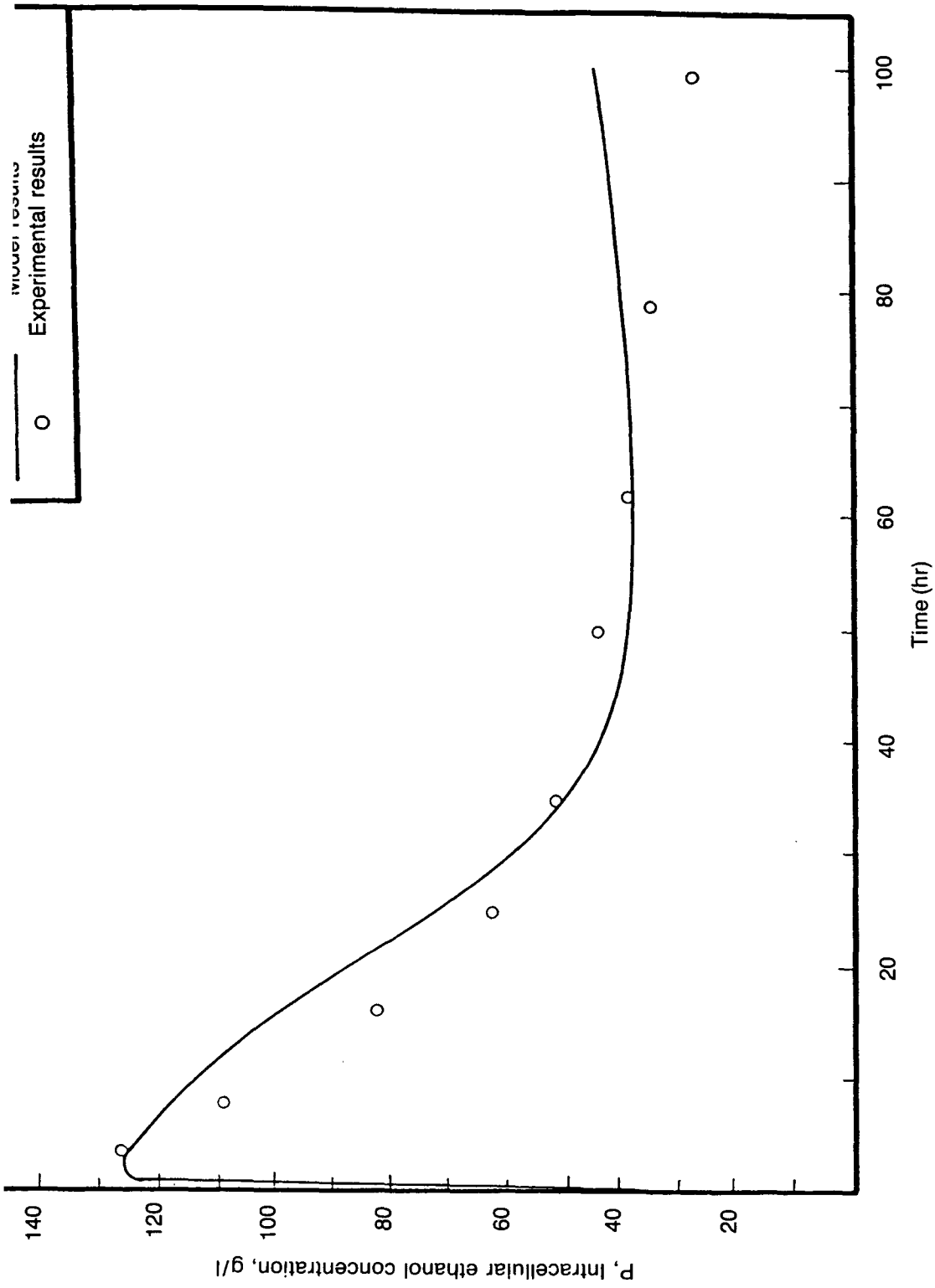

Fig. 9. Solution of the heterogeneous model using intermediate K_p value, variable ethanol permeability, cell inhibition effect, and two independent rate equations. Intracellular ethanol concentration vs time.

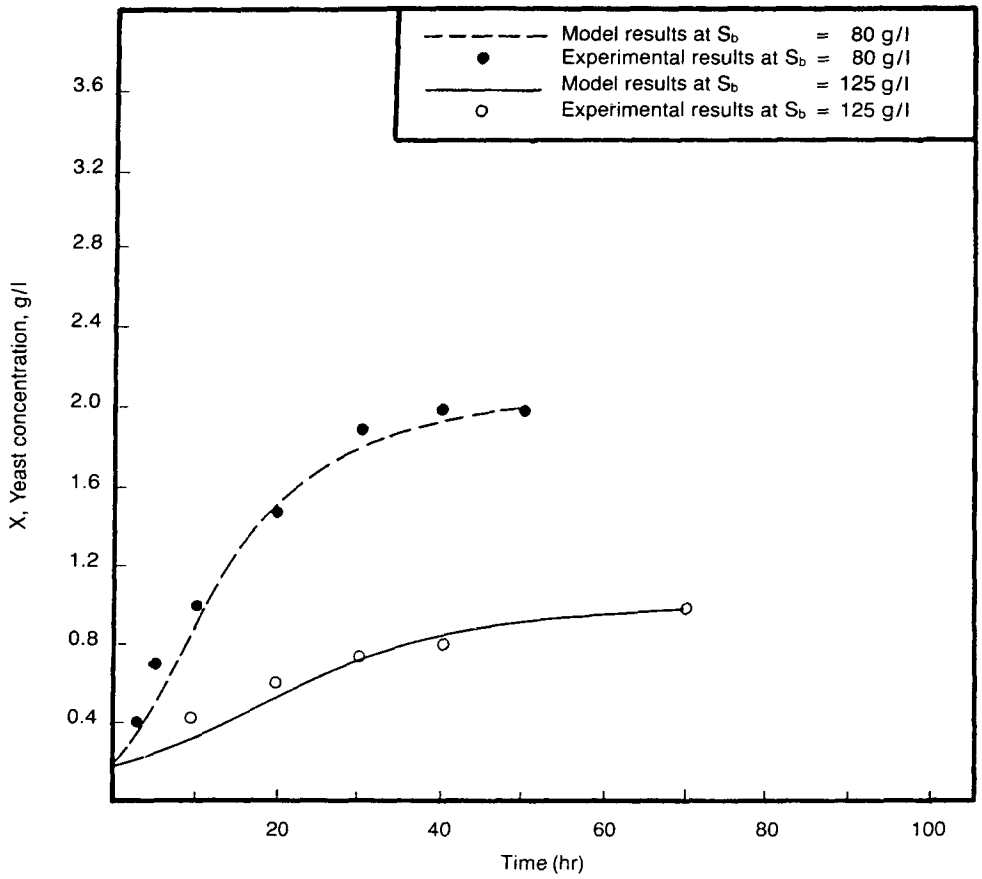

Fig. 10. Comparison between the model and the experimental results using the heterogeneous model at $S_{bo}=80$ g/L and $S_{bo}=125$ g/L. Biomass concentration vs time. — — — Model results for $S_{bo}=80$ g/L. ●●● Experimental results for $S_{bo}=80$ g/L. ———— Model results for $S_{bo}=125$ g/L. ○○○ Experimental results for $S_{bo}=125$ g/L.

validity of this heterogeneous model for the simulation of the fermentation process.

Initial Conditions of the Anarobic Period

Data obtained from the plant

Biomass concentration	$X_o = 1.0$ g dry wt/L
Extracellular ethanol concentration	$P_{bo}=25$ g/L
Extracellular sugar concentration	$S_{bo}=59$ g/L
Initial liquid volume	$V_o = 36000$ L
Final total volume of the contents of the fermentor (at the end of the feeding period)	$V_t = 65000$ L
Volumetric feed flow rate	$Q = 2500$ L/h
Sugar concentration in feed stream	$S_f = 152$ g/L

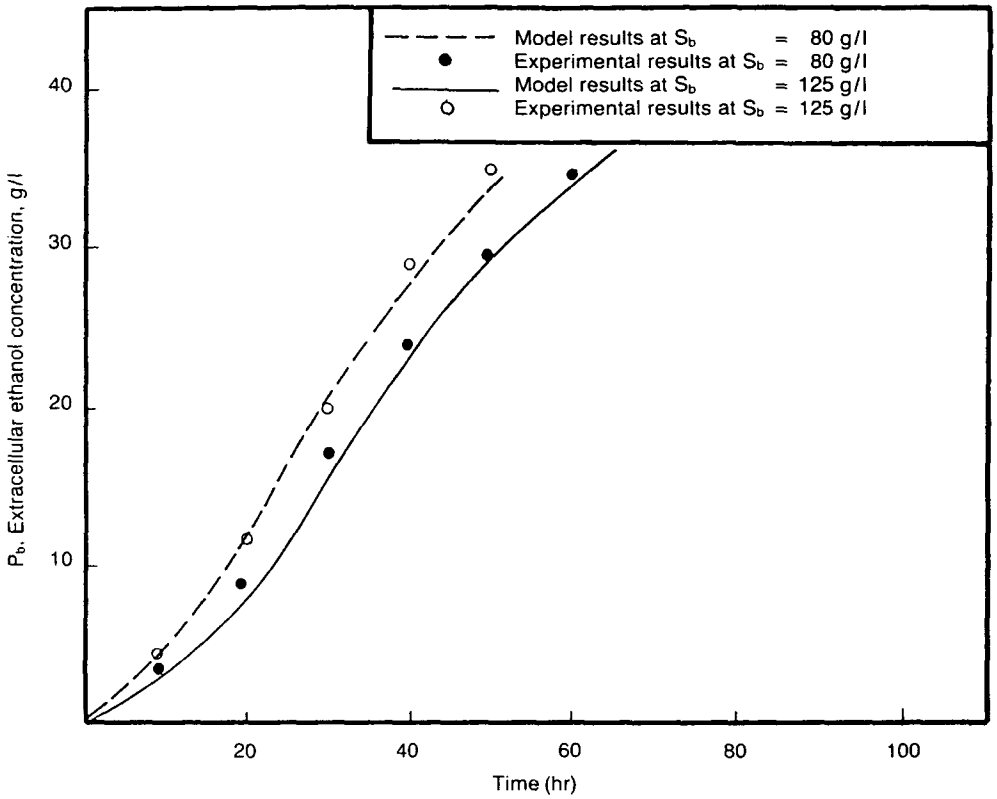

Fig. 11. Comparison between the theoretical and the experimental results using the heterogeneous model at $S_{bo}=80$ g/L and $S_{bo}=125$ g/L. Extracellular ethanol concentration vs time. — — — Model results for $S_{bo}=80$ g/L. ● ● ● Experimental results for $S_{bo}=80$ g/L. ———— Model results for $S_{bo}=125$ g/L. · · · · Experimental results for $S_{bo}=125$ g/L.

The initial intracellular concentration of sugar and ethanol at the beginning of the anarobic period are necessary to solve the heterogeneous model equations. These were estimated to be

Intracellular ethanol concentration	$P_p = 50$ g/L
Intracellular sugar concentration	$S_o = 55$ g/L

Kinetic and Physical Parameters

The same parameters in Table 1 are used except the following values that were obtained from plant data

$Y_p = 0.45$
$Y_c = 0.01$
$X_m = 2.5$
$D_p = 0.001$ cm

The difference here is owing to the plant using yeast strain different than that used by Novak (*1*).

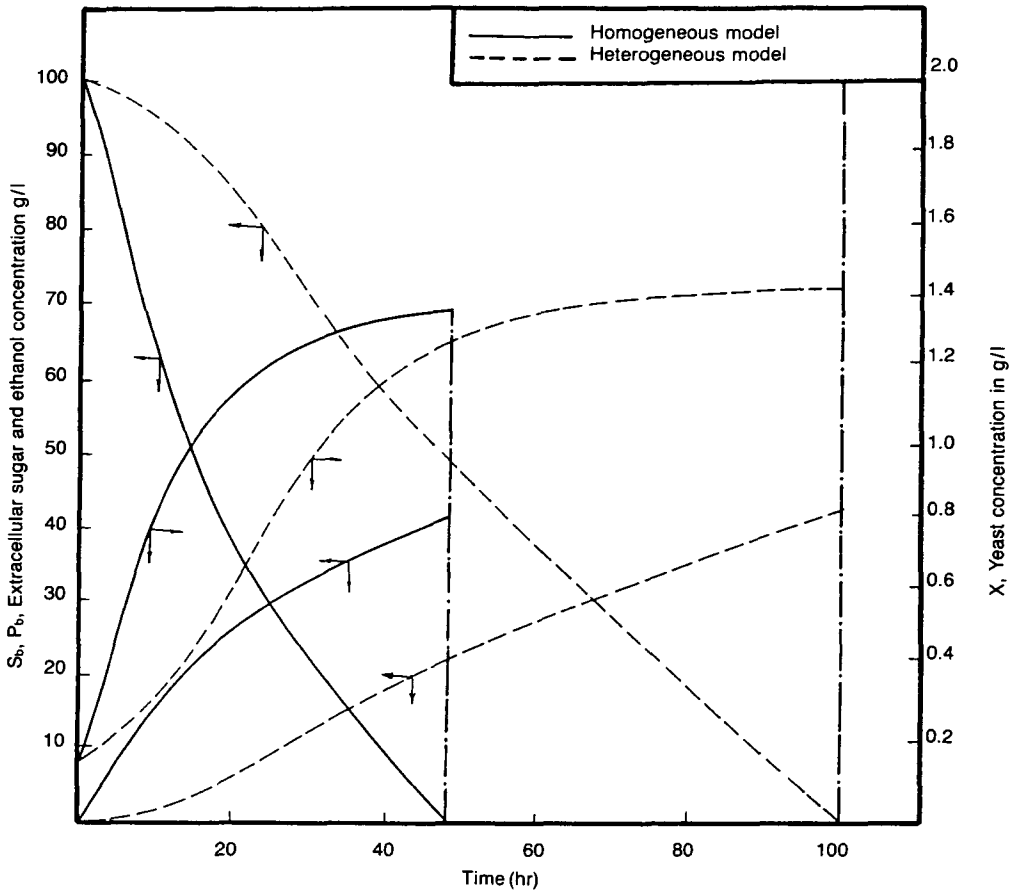

Fig. 12. A comparison between the homogeneous and the heterogeneous model.

Plant Final Conditions

The final sugar conversion in the plant was 98% of the fermentable sugar, for anarobic fermentation time ranging from 18–20 h. The output composition is: Extracellular sugar (fermentable) concentration ranges from 2–3 g/L. Extracellular ethanol concentration ranges from 50–60 g/L. Biomass concentration ranges from 1.1–1.3 g dry wt/L.

COMPARISON BETWEEN THE MODEL PREDICTION AND PLANT PERFORMANCE

Figures 13–15 present the solution of the heterogeneous model. Figure 13 represents the variation of the extracellular sugar concentration vs time. It is shown that the model predicts the anarobic fermentation time required to achieve about 98% conversion as 19.4 h. This compares very well with

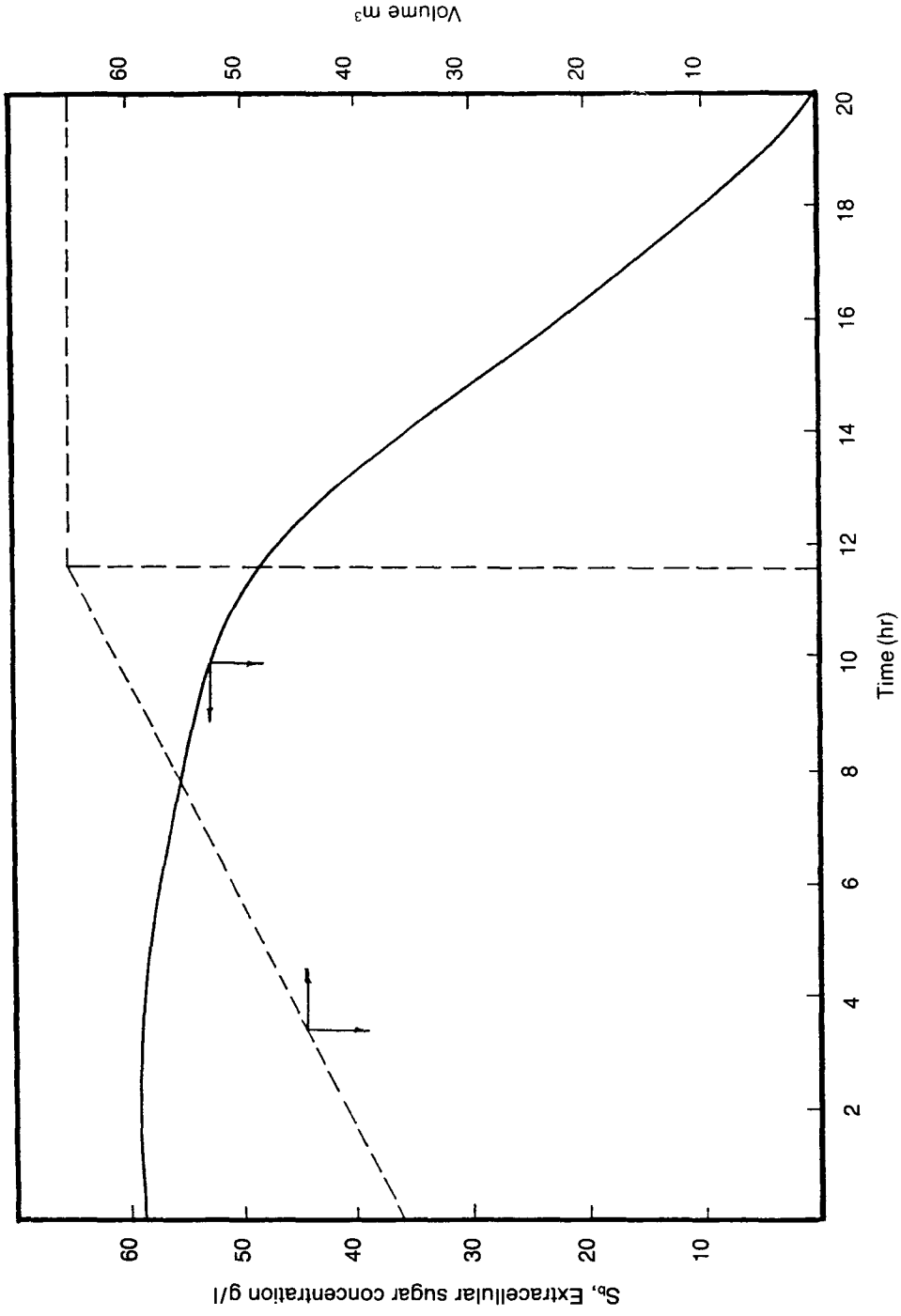

Fig. 13. Simulation of the industrial fed-batch fermentor. Extracellular sugar concentration vs time.

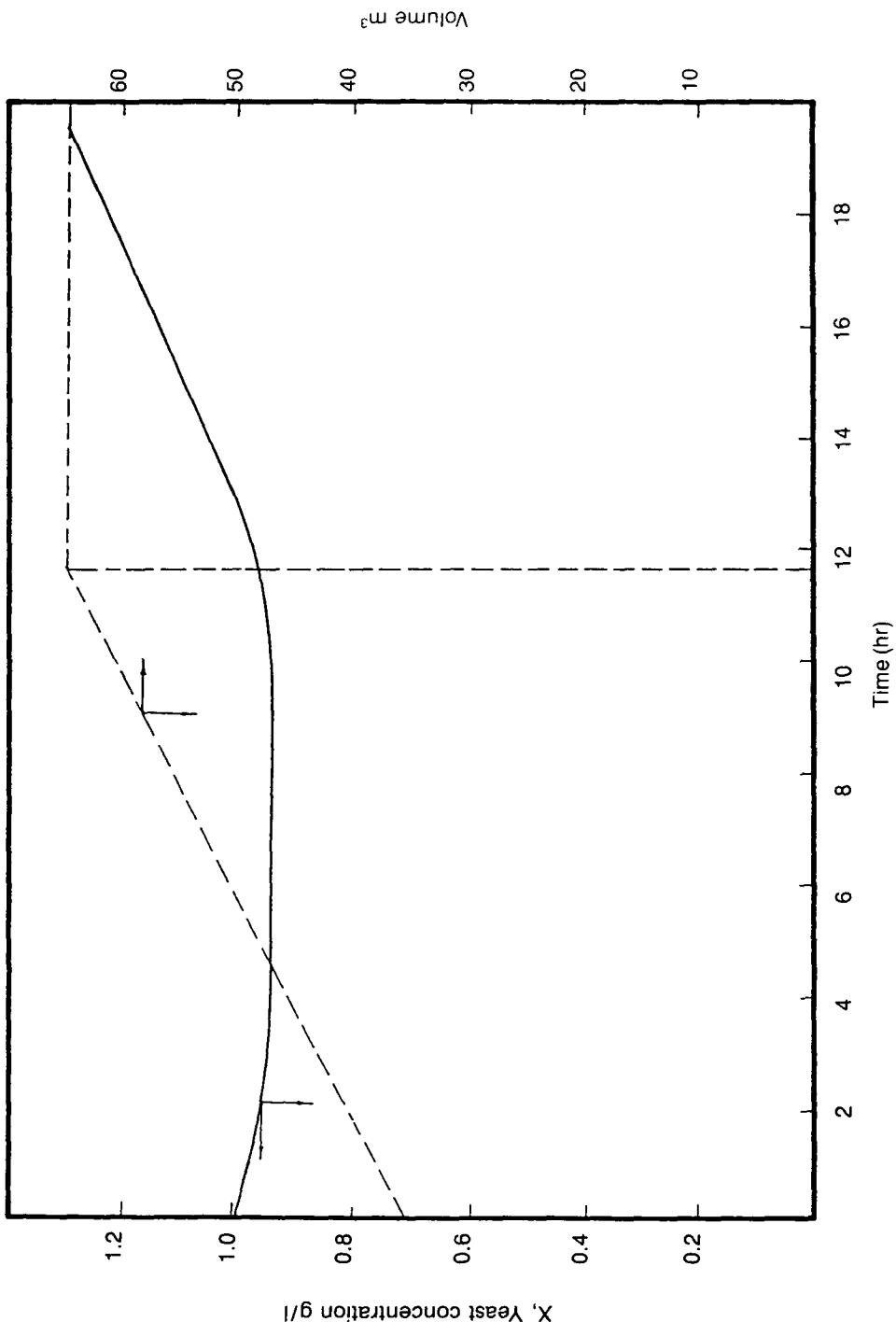

Fig. 14. Simulation of the industrial fed-batch fermentor. Biomass concentration vs time.

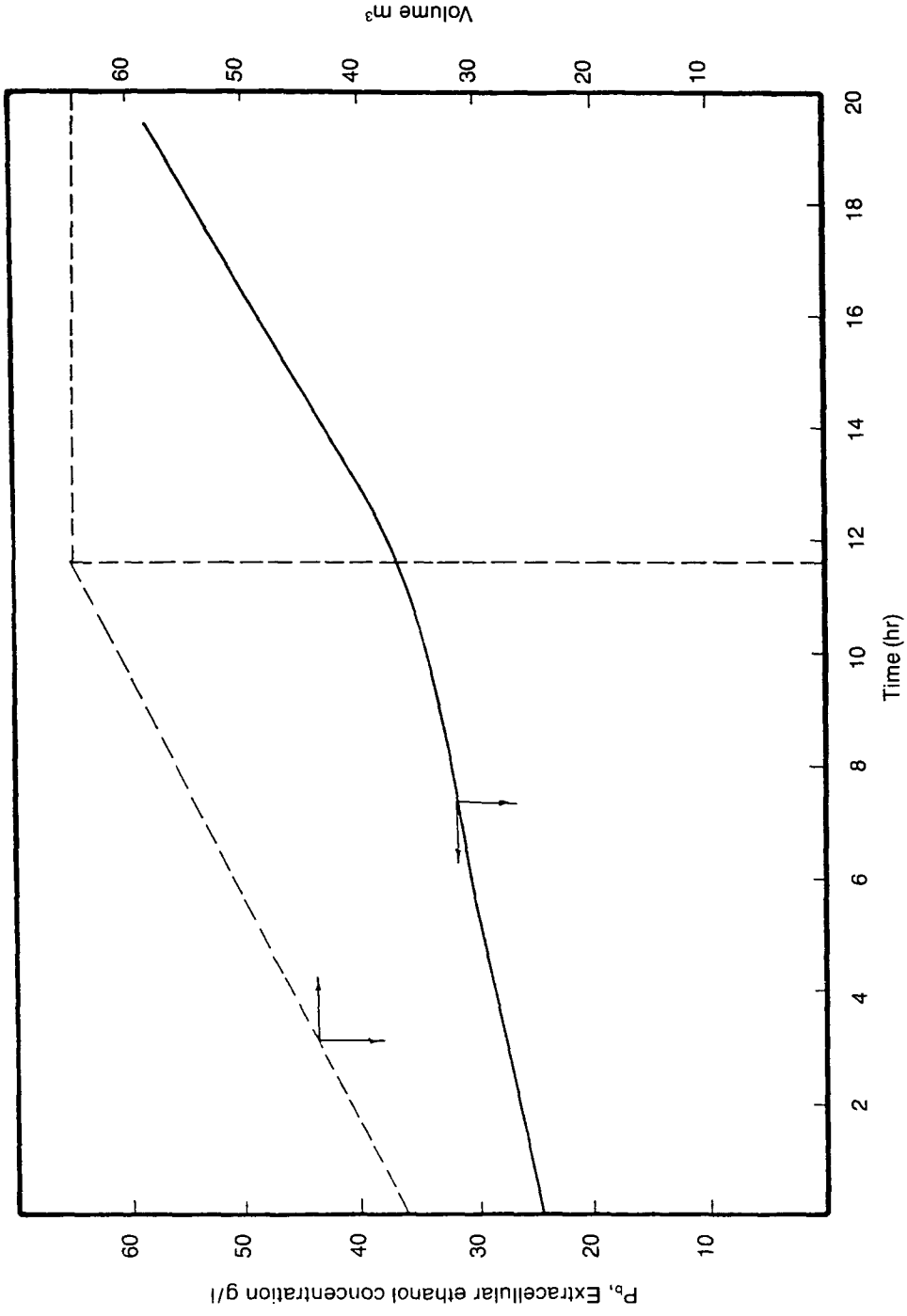

Fig. 15. Simulation of the industrial fed-batch fermentor. Extracellular ethanol concentration vs time.

the actual industrial fermentor where the anarobic fermentation time for the different batches in the plant ranged from 18 to 20 h. For the period of continuous feeding, the extracellular sugar concentration decreases at very slow rate. This is owing to the continuous feeding of fresh sugar solution (*46*). The advantage of using this mode of operation (fed-batch) is to operate under relatively low sugar concentration to avoid the inhibitory effect of sugar and ethanol (*47–48*).

Figure 14 represents the variation of biomass concentration vs time. It is observed numerically from the model solution that a slight decrease in biomass concentration (from 1 g dry wt/L to 0.93 g dry wt/L) takes place in the first period, then the biomass concentration increases in the second period (batch period). This slight decrease of biomass concentration at the beginning is owing to the fact that the produced biomass could not elevate its concentration markedly in this first period because of the continuous dilution. The final biomass concentration that corresponds to about 98% conversion is about 1.28 g dry wt/L. This value confirms quite well with the actual fermentor results where the final biomass concentration ranged from 1.1 g/L to 1.3 g/L.

Figure 15 represents the variation of the extracellular ethanol concentration vs time. It is observed that, for the first period (feeding period) the ethanol concentration increases very slowly, whereas for the second period (batch period) it increases relatively fast. The final ethanol concentration that corresponds to about 98% conversion is shown to be about 57.8 g/L. This agrees well with the actual fermentor results where the final concentration of ethanol ranges from 50 to 60 g/L. On the other hand, Fig. 16 shows the response of both the pseudohomogeneous and the heterogeneous model.

It is evident that the fermentation time predicted by the use of the pseudohomogeneous model is lower than that predicted by the heterogeneous model. For 98% conversion the pseudohomogeneous model predicts a time of about 15 h, whereas the heterogeneous model predicts 19.4 h. With respect to the batch period (after 11.6 h of the feeding period) the time predicted by the use of the homogeneous model is about 3.4 h, whereas the time predicted by the use of the heterogeneous model is about 7.8 h. The actual time for the batch period of the industrial fermentor is 6.4–8.4 h. It is clear that the pseudohomogeneous model overestimates the rates of reaction since it neglects mass transfer limitations, whereas the heterogeneous model developed reasonably well simulates the complex diffusion-reaction process taking place in the fermentor.

CONCLUSIONS

The heterogeneous model developed for the fermentation process was found to represent quite well the fermentation process for laboratory fermentors as well as industrial fed-batch fermentors. Although some of

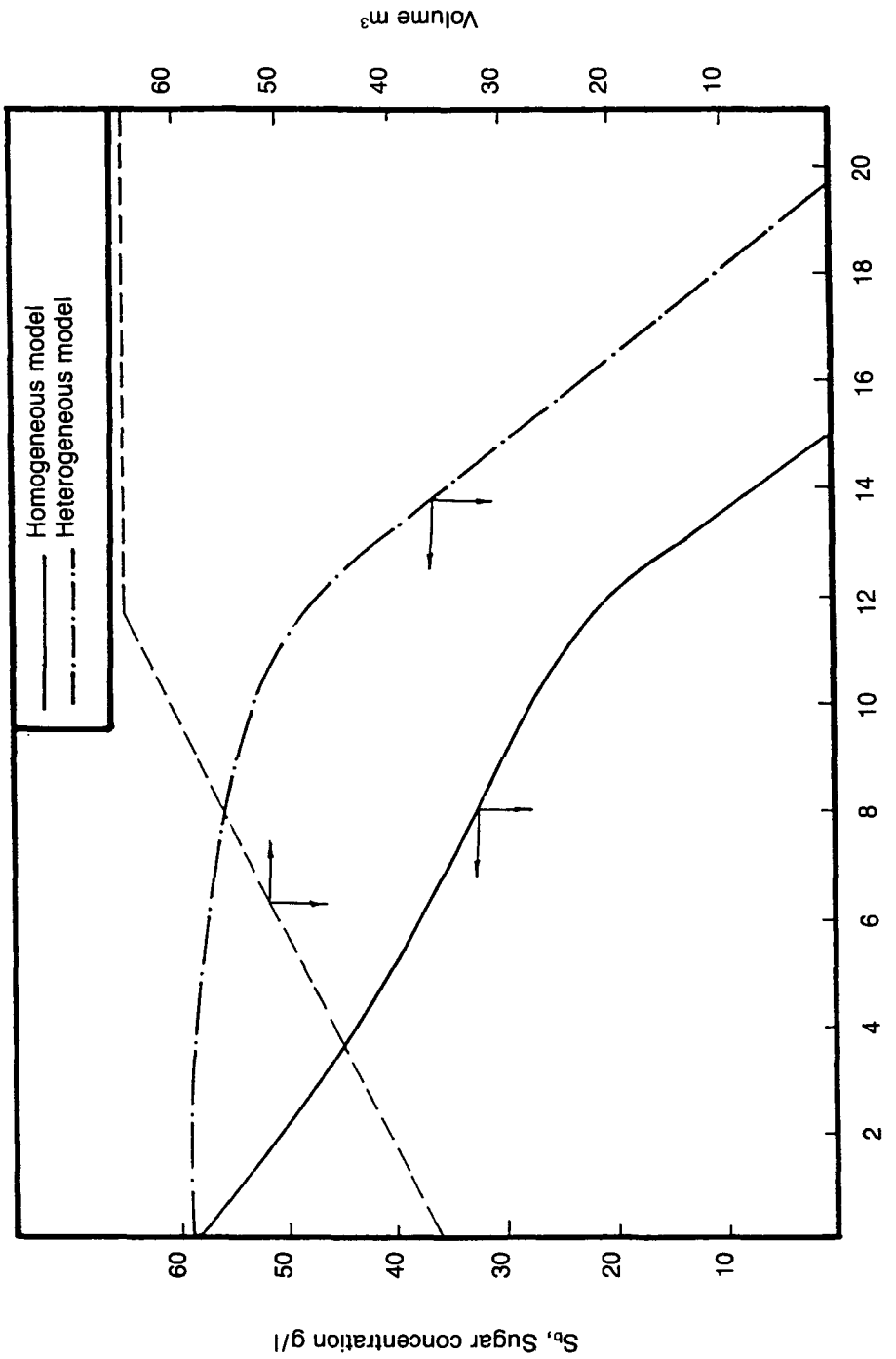

Fig. 16. Comparison between the homogeneous and the heterogenous models for the industrial fed-batch fermentor.

the model parameters are obtained by fitting the model to one set of experimental results, the excellent results obtained using the model for the simulation of other experimental results and an industrial fed-batch fermentor gives the model and its parameters more general value than empirical models.

Of course, we are still a long distance from complete rigorous simulation of diffusion with biochemical reactions in the fermentation process, which may need a complex structured model and certainly more information about what is happening at the cell membrane. The present model can easily be extended to cases where the yeast is immobilized (*50,51*).

The model can also be used to obtain a more realistic optimal policy for fed-batch fermentors than the policies obtained using psuedohomogeneous models (*52*). The procedure for optimal control of reactors using heterogeneous models that take into consideration intraparticle diffusional limitation has been recently developed by Elnashaie and Abdel-Hakim (*53*).

ACKNOWLEDGMENT

The authors would like to acknowledge the great help given to them by the entire staff of the Egyptian Sugar and Refinery Company, El-Hawamdia Factory. The authors would also like to report their appreciation to the reviewer of the paper for some very useful criticisms that contributed positively to the paper.

REFERENCES

1. Novak, M., Strehaiano, P., Moreno, N., and Goma, G. (1981), *Biotech. Bioeng.*, **23,** 201–211.
2. Bailey, J. E. and Ollis, D. F. (1986), *Biochemical Engineering Fundamentals,* 2nd ed., McGraw Hill.
3. Ghose, T. K. and Tyagi, R. D. (1979), *Biotech. Bioeng.*, **22,** 1387–1400.
4. Holzberg, I., Finn, R. K., and Stienkraus, K. H. (1967), *Biotech. Bioeng.*, **9,** 413–427.
5. Aiba, S., Shoda, M., and Nagatani, M. (1968), *Biotech. Bioeng.*, **10,** 845–864.
6. Egamberdiev, N. B. and Ierusalimskij, N. D. (1969), "In continuous Cultivation of Micro-organism.I," Malek et al., eds., Academic, Praha, 517–527.
7. Levenspiel, O. (1980), *Biotech. Bioeng.*, **22,** 1671–1687.
8. Roels, J. A. and Kossen, N. W. F. (1978), *Progress in Industrial Microbiology,* H. J. Bull, ed., Elsevier, Amsterdam, 95–203.
9. Nagodawithana, T. W., Whitt, J. T., and Cutaia, A. J. (1977), *J. Am. Soc. Brew. Chem.*, **35,** 179.
10. Leao, C. and Van Uden, N. (1982), *Biotech. Bioeng.*, **24,** 2601.
11. Jobses, I. M. L. and Roels, J. A. (1986), *Biotech. Bioeng.*, **28,** 554–563.

12. Ghose, T. K. and Tyagi, R. D. (1979), *Biotech. Bioeng.*, **22,** 1401–1420.
13. Franz, B. (1961), *Die Nahorung*, **5,** 457.
14. Pioronti, F. (1971), Ph.D. thesis, Cornell University, Ithaca, NY.
15. Egamberdiev, N. B. and Ierusalimskij, N. D. (1968), *Microbiologiya*, **37,** 686.
16. Burger, M., Hejmova, L., and Kleizeller, A. (1959), *Biochem. J.*, **71,** 497.
17. Ciftci, T., Constantinides, A., and Wang, S. S. (1983), *Biotech. Bioeng.*, **25,** 2007–2023.
18. Cysewski, G. R. and Wilke, C. R. (1978), *Biotech. Bioeng.*, **20,** 1421.
19. Lee, J. M., Pollard, J. F., and Coulman, G. A. (1983), *Biotech. Bioeng.*, **25,** 497–511.
20. Nagodawithana, T. W. and Steinkrous, K. H. (1976), *J. Appl. Environ. Microbiol.*, **31,** 158.
21. Thomas, D. S. and Rose, A. H. (1979), *Arch. Microbiol.*, **122,** 49.
22. Beavan, M. J., Charpentier, C., and Rose, A. H. (1982), *J. Gen. Microbiol.*, **128,** 1447.
23. Navarro, J. M. and Durand, G. (1978), *Ann. Microbiol.* (Inst. Pasteur), **129B,** 215.
24. Navarro, J. M., Scherian, A. F., Weiland, P., and Lafferty, R. M. (1981), Paper presented at the 7th International Specialized Symposium on Yeast, Valencia, Spain.
25. Panchal, J. and Stewart, G. G. (1980), *J. Inst. Brew.*, **86,** 207.
26. Strehaiano, P. (1973), These Dr. Ing., Toulouse, France.
27. Guijarro, J. M. and Lagunas, R. (1984), *J. Bacteriol.*, **160,** 3, 874–878.
28. Benitez, T., Del Castillo, L., Aguilera, A., Conde, J., and Cerda-Omeda, E. (1983), *Appl. Environ. Microbiol.*, **45,** 1429–1439.
29. Aris, R. (1975), *The Mathematical Theory of Diffusion and Reaction in Permeable Catalyst*, Oxford Univ. Press, vols. 1 and 2.
30. Dombek, K. M. and Ingram, L. O. (1983), *Abstr. Ann. Meet. Soc. Microbiol.*, **83,** meeting 241.
31. Carey, V. C. and Ingram, L. O. (1983), *J. Bact.*, **154,** 1291.
32. Bajpai, P. and Margaritis, A. (1986), *Biotech. Bioeng.*, **28,** 283–287.
33. Mill, P. J. (1964), *J. Gen. Microbiol.*, **35,** 61.
34. Atkinson, B. and UR-Rahman, F. (1979), *Biotech. Bioeng.*, **21,** 221–251.
35. Stein, W. D. (1967), *The Movement of Molecules Across Cell Membranes*, Academic, NY, London.
36. Weeks, M. G., Munro, P. A., and Speeding, P. L. (1983), *Biotech. Bioeng.*, **25,** 687–698.
37. Weeks, M. G., Munro, P. A., and Speeding, P. L. (1983), *Biotech. Bioeng.*, **25,** 699.
38. Atkinson, B. and Daoud, I. S. (1976), *Advances in Biochemical Engng.*, **4,** T. K. Ghosh, A. Fiechter, N. Blakeborough, eds., Springler-Verlag, Berlin.
39. Eddy, A. A. (1955), *J. Inst. Brew.*, **61,** 313.
40. Baker, D. A. and Kirsop, B. H. (1972), *J. Inst. Brew.*, **78,** 454.
41. Rainbow, C. (1966), *Process Biochem.*, **1,** 489.
42. Jones, S. T., Korus, R., Adamssu, W., and Hemisch, R. C. (1984), *Biotech. Bioeng.*, 742–747.
43. Ibrahim, G. (1986), *The Analysis and Design of Fermentors for the Production of Alcohol*, Ph.D. thesis, Chem. Engng. Dept., Cairo University, Egypt.
44. Virgillio, L. and Ferreiva, H. G. (1983), *Biotech. Bioeng.*, **25,** 2263–2269.

45. Luong, J. H. T. (1985), *Biotech. Bioeng.*, **27**, 280–285.
46. Del Rosario, E. J., Lee, K. J., and Rogers, P. L. (1979), *Biotech. Bioeng.*, **21**, 1477–1482.
47. Silman, R. W. (1984), *Biotech. Bioeng.*, **26**, 247–251.
48. Jobses, I. (1986), Ph.D. thesis, Delft Univ. of Technology, The Netherlands, p. 56.
49. Atkinson, B. (1971), *Biochemical Reaction Engineering in Chem. Eng.*, vol. 3, Coulson, J. M. and Richardson, J. F., eds., Pergamon, Oxford, p. 347.
50. Gancer, M. A. and Mutharsan, R. (1983), *Biotech. Bioeng.*, **25**, 2243–2262.
51. Nagshima, M., Azuma, M., Noguchi, S., Inzuka, K., and Samejima, H. (1984), *Biotech. Bioeng.*, **26**, 992–997.
52. San, K. Y. and Stephanopoulos, G. (1984), *Biotech. Bioeng.*, **26**, 1261–1264.
53. Elnashaie, S. S. E. H. and Abdel Hakim, N. (in press), *Computers & Chem. Engng.*

APPENDIX 1

Method of Estimation and Correlation of Ethanol Mass Transfer Coefficient

The experimental data (Table A.I) that this work aims to simulate involves the variation of sugar concentration in the bulk phase (S_b), extracellular as well as intracellular ethanol concentrations (P and P_b), and the biomass concentration (X) through the time course of batch fermentation.

The method used to estimate the mass transfer coefficient for ethanol depends on the knowledge of S_b, P_b, P, and X variation with time. Table (A.I) together with Eq. (17)

$$dP_b / dt = 6.X.K_{gp} (P - P_b) / D_p (\rho - X)$$

can be used to estimate K_{gp} at different values of t, i.e., at different values of S_b.

Table A.I.
Variation of Ethanol Permeability with Time for Novak et al. (*1*)
First Set of Experimental Data

Time	S_b, g/L	P_b, g/L	X, g/L	P, g/L	K_{gp}, dm/h
4	98.0	0.9	0.2	127	1.0836×10^{-4}
8	94.6	1.0	0.34	108	1.4508×10^{-4}
16	87.0	4.0	0.7	82	2.4732×10^{-4}
18	83.0	5.4	0.76	77	2.7792×10^{-4}
25	71.0	9.0	0.91	62	4.356×10^{-4}
35	59.0	14.0	1.04	52	6.732×10^{-4}
50	48.0	21.4	1.16	44	12.42×10^{-4}
62	37.0	27.0	1.28	40	22.536×10^{-4}

The only disadvantages of this technique for estimating K_{gp} is that it needs the evaluation of the slope (dP_b / dt) at the different points from a curve drawn with a limited number of points, which may lead to numerical error. To check the results obtained from this method K_{gp} was computed at the different points using another method based on assuming pseudo-steady states at the different points (*43*). The results of both methods were very close and thus we considered them to be the best possible representation for the variation of the ethanol mass transfer coefficient at the present state of knowledge with regard to diffusion through the cell membrane.

In order to correlate the values of K_{gp} at each data point with the sugar concentration, the best fit for data in Table A.I was obtained by the formula

$$K_{gp} = a_0 + a_1 S_b + a_2 S_b^2 + a_3 S_b^3 \qquad \text{(A.I)}$$

where

$$a_0 = 0.01071204,$$
$$a_1 = -3.6675 * 10^{-4}$$
$$a_2 = 0.43937 * 10^{-5},$$
$$a_3 = -1.79293 * 10^{-8}$$

APPENDIX 2

Method of Determination of the Mean Floc Size of the Industrial Strain

An approximation to the mean floc size may be obtained from a photomicrograph of the floc. The photomicrograph of the flocs has shown that the average number of yeast cells involved in the floc is about ten cells. Taking the amplification ratio into consideration the cell diameter for the fed-batch industrial fermentor has a value of about 0.000045 dm. The procedure followed was

Cell volume $= (4/3)\ \pi\ R_c^3 = 4.773 * 10^{-14}\ dm^3$
Floc volume = average number of cells × cell volume
$= 10 * 4.773 * 10^{-14}\ dm^3$
Floc diameter $= 2\ (\text{floc volume} \times (3/4\pi))^{1/3} = 0.969 * 10^{-4} dm$

The average floc diameter used for the industrial fed-batch fermentor is taken to be equal to $1 * 10^{-4}$ dm. The average floc diameter for the simulation of Novak et al. (*1*) results is equal to $5 * 10^{-4}$ dm because of the absence of antiflocculating agents.